

# Phase transitions in a ferrofluid at magnetic-field-induced microphase separation

D. Lacoste and T. C. Lubensky

*Department of Physics, University of Pennsylvania, Philadelphia, Pennsylvania 19104-6396*

(Received 20 March 2001; published 24 September 2001)

In the presence of a magnetic field applied perpendicular to a thin sample layer, a suspension of magnetic colloidal particles (ferrofluid) can form spatially modulated phases with a characteristic length determined by the competition between dipolar forces and short-range forces opposing density variations. We introduce models for thin-film ferrofluids in which magnetization and particle density are viewed as independent variables and in which the nonmagnetic properties of the colloidal particles are described either by a lattice-gas entropy or by the Carnahan-Starling free energy. Our description is particularly well suited to the low-particle-density regions studied in many experiments. Within mean-field theory, we find isotropic, hexagonal and stripe phases, separated in general by first-order phase boundaries.

DOI: 10.1103/PhysRevE.64.041506

PACS number(s): 47.54.+r

## I. INTRODUCTION

Ferrofluids are suspensions of ferromagnetic particles with a diameter of about 10 nm in a carrier fluid. The particles are stabilized against aggregation by coating with polymers for oily ferrofluids or with charged surfactant for aqueous ferrofluids. On macroscopic scales, ferrofluids can be described as superparamagnetic liquids [1]. The application of a magnetic field perpendicular to a thin layer induces microphase separation in a homogeneous aqueous or oily ferrofluid with no surfactant and leads to the formation of a periodic lattice of unbranched [2,3] or branched [4] concentrated phase columns. In thin layers of ferrofluid confined together with an immiscible nonmagnetic liquid, the columns can merge into sheets [5], and at a higher field, the sheets evolve into a disordered labyrinthine structure [1]. In pure ferrofluids and in ferrofluid emulsions, only the hexagonal phase of columns has been reported [6]. Similar periodic structures have been observed in other physical systems such as Langmuir monolayers [7], magnetic garnet thin films [8], or type I superconductors [9], as discussed by Seul and Wolfe [10]. In all these systems, there is a spontaneous spatial modulation of an order parameter, which can be either the concentration or the magnetization of the particles, or a combination thereof. The period of the modulation is determined by the competition between long-range dipolar forces and short-range forces favoring constant density. It depends on the magnetic field and the thickness of the sample layer as discussed in a recent study on the aggregate size and spacing formed in a thin film of ferrofluid [11].

This paper concerns the thermodynamic stability and pattern formation in a suspension of ferromagnetic particles in a carrier fluid in the presence of a magnetic field applied perpendicular to the sample layer. We formulate models for thin films of these suspensions in which particle concentration and magnetization, determined by the degree of alignment of magnetic moments as well as particle concentration, are treated as independent variables. We discuss two possible models for the entropy of the fluid, the lattice gas model and the Carnahan-Starling model [12]. Although the Carnahan-Starling model has already been used for magnetic fluids [13], it has not been used to describe transitions from a dis-

ordered to an ordered phase in ferrofluids. Our lattice model is essentially identical to that of Sano and Doi [14] except that we consider the complete wave-number dependence of interactions rather than the infinite wave-number limit appropriate to needlelike magnetic domains. Several previous studies, including those of Andelman *et al.* [7] and Cebers [15,16], are based on Landau expansion of a lattice-gas model in the vicinity of the liquid-gas critical point present in the absence of the long-range part of the dipolar interactions. The free energies of these models are even-order expansions up to fourth order in the deviation of the local density (which includes the modulated and spatially uniform components) from the liquid-gas critical density. Our model free energy is in principle valid for arbitrary values of the spatially uniform part of the particle density. We place no restrictions on the spatially uniform components of the density, but we do expand the free energy in a power series in the spatially varying component of the density. The entropy of the lattice-gas model is invariant under  $(\phi - \frac{1}{2}) \rightarrow -(\phi - \frac{1}{2})$ , where  $\phi$  is the volume fraction of ferrofluid particles. The Carnahan-Starling entropy possesses no such symmetry. As a result, its phase diagram, as we shall see, is more asymmetric than that of the lattice-gas model, and its interesting features occur at  $\phi < 1/2$ . We investigate the phase diagrams of our model within mean-field theory in which modulated hexagonal and stripe phases are described by sine waves with wave numbers of a fixed magnitude. Our results are in qualitative agreement with those of Cebers [15,16] and of Halsey [17] but differ from them in detail, particularly in the low-density regions in which nonmagnetic interactions are best described by the Carnahan-Starling free energy.

## II. HELMOLTZ FREE ENERGY

The magnetic particles are assumed to have a spherical ferromagnetic core of radius  $a$ , coated by a sheath of surfactant  $\delta$ . Due to steric hindrance, the particles cannot come closer than a distance  $d = 2(a + \delta)$ . Each particle of the ferrofluid is a magnetic single domain of magnetic moment

$$m_0 = \frac{4\pi}{3} a^3 M_s \mu_0, \quad (1)$$

where  $M_s$  is the saturation magnetization of the bulk material and  $\mu_0$  is the magnetic permeability of the vacuum. The volume of the particles is  $v_0 = \pi d^3/6$ . It is assumed that the suspension is monodisperse and that each particle carries the same magnetic moment. We define  $m(\mathbf{r})$  to be the ratio of the average magnetic moment divided by  $m_0$ , so that  $0 \leq m \leq 1$ , and  $\phi(\mathbf{r})$  to be the volume fraction of the ferrofluid at point  $\mathbf{r}$ . We treat the particles as hard spheres, and we include only magnetic dipolar interaction beyond hard sphere repulsion.

The total free energy  $F$  of the ferrofluid in a magnetic field breaks up into four main contributions: the free energy of independent magnetized particles in a magnetic field  $F_m(m, \phi)$ , the dipolar interaction energy  $E_{dip}(m, \phi)$ , the entropic contribution of the hard spheres fluid, and the energy cost associated with deviations of  $\phi$  from spatial uniformity  $F_{nu}(\phi) = k_B T L A \int d^2 \mathbf{r} (\nabla \phi)^2 / (2v_0)$ . In this last term,  $L$  is the thickness of the slab and  $A$  is a parameter with units of the square of a length, independent of the magnetic field, which is related to the structure factor at low scattering angle [18]. In the absence of a magnetic field,  $A$  is negative for an hard sphere fluid [19]. As will become clear later, there are no stable long wavelength stripes if  $A$  is negative. We therefore assume in this paper that  $A$  is positive, either because of local field contributions or because of attractive interactions.

We have used two different forms of the entropy: the entropy of a gas on a lattice, which has the following form per site

$$s(\phi) = \phi \ln \phi + (1 - \phi) \ln(1 - \phi), \quad (2)$$

and the entropy

$$s(\phi) = \phi \left[ \ln \phi + \phi \frac{4 - 3\phi}{(-1 + \phi)^2} \right] \quad (3)$$

of a Carnahan-Starling fluid [12]. In the absence of further interactions, the free energies  $-k_B T s(\phi)$  of these models are convex, and their equilibrium stable phase is a single-phase fluid with spatially uniform  $\phi$ . As can be seen from Eqs. (2) and (3), the entropy of the lattice model is an even function of  $\phi - 0.5$ , whereas the entropy of the Carnahan-Starling fluid does not have this symmetry. The function  $F_m$  follows from a Langevin approach [see Appendix A for the derivation],

$$\frac{F_m}{k_B T} = \frac{L}{v_0} \int d^2 \mathbf{r} \phi [f_m(m) - mh], \quad (4)$$

with

$$f_m(m) = m \mathcal{L}^{-1}(m) - \ln \left\{ \frac{\sinh[\mathcal{L}^{-1}(m)]}{\mathcal{L}^{-1}(m)} \right\}, \quad (5)$$

with  $\mathcal{L}^{-1}$  denoting the inverse of the Langevin function. The second term in Eq. (4) is the energy of the dipoles in the magnetic field  $h$  and the first term, the function  $f_m(m)$ , represents the rotational entropy of the dipoles. In Eq. (4), we have introduced

$$h = \frac{H m_0}{k_B T}, \quad (6)$$

which is a unitless measure of the external magnetic field  $H$ .

The dipolar interaction energy (in SI units) can be written generally as

$$E_{dip} = \frac{m_0^2}{8 \pi \mu_0} \sum_{\alpha, \beta} m_\alpha^i m_\beta^j \left( -\nabla_i \nabla_j \frac{1}{|\mathbf{r}_\alpha - \mathbf{r}_\beta|} \right), \quad (7)$$

where  $i$  and  $j$  are Cartesian coordinates, and  $m_\alpha$  ( $m_\beta$ ) is the dimensionless magnetic moment of the particle located at the point  $\mathbf{r}_\alpha$  ( $\mathbf{r}_\beta$ ). Since  $\mathbf{m}_\alpha$  represents an angular average of the dipole moment, it is directed along the  $z$  axis, which is taken to be the direction of the applied magnetic field. In the following, we will assume that  $\mathbf{m}_\alpha = m_\alpha \mathbf{e}_z$  is independent of the  $z$  coordinate. In a continuous description of the medium, which will be discussed in the next section, the local magnetization is

$$M(\mathbf{r}) = m_0 m(\mathbf{r}) \frac{\phi(\mathbf{r})}{v_0}, \quad (8)$$

where  $m(\mathbf{r})$  is the coarse-grained unitless magnetic moment at  $\mathbf{r}$ . Inserting this equation into the continuum limit of Eq. (7) gives

$$\frac{E_{dip}}{k_B T} = \frac{\tilde{\lambda} L}{2v_0} \int d^2 \mathbf{r} d^2 \mathbf{r}' \phi(\mathbf{r}) \phi(\mathbf{r}') m(\mathbf{r}) m(\mathbf{r}') g(\mathbf{r}, \mathbf{r}'), \quad (9)$$

where  $\tilde{\lambda}$  is a measure of the dipole-dipole interaction,

$$\tilde{\lambda} = 24\lambda,$$

with

$$\lambda = \frac{m_0^2}{4 \pi \mu_0 d^3 k_B T} = \frac{\mu_0 M_s^2 4 \pi a^6}{9 d^3 k_B T}, \quad (10)$$

where  $\lambda$  is the parameter introduced by de Gennes and Pincus [21]. The two-dimensional (2D) Fourier transform of the function  $g(\mathbf{r}, \mathbf{r}')$  present in Eq. (9) is defined as

$$g(\mathbf{r}, \mathbf{r}') = \int \frac{d^2 \mathbf{q}}{(2\pi)^2} g(\mathbf{q}) e^{i\pi \mathbf{q} \cdot (\mathbf{r} - \mathbf{r}')}. \quad (11)$$

It depends only on  $q = |\mathbf{q}|$  and it takes the form

$$g(q) = \frac{1}{qL} [1 - \exp(-qL)] - \frac{1}{3}, \quad (12)$$

which can be interpreted as the dipolar part of the pair correlation function [21,8]. The first term in Eq. (12) is the long-range contribution of the interaction, which tends to 1, the demagnetizing factor of a film as  $q \rightarrow 0$  and to 0, the demagnetizing factor of a needle as  $q \rightarrow \infty$ . The second term is the short-range contribution due to the local field induced by the surrounding magnetic dipoles. In this geometry where the applied magnetic field is perpendicular to the sample

layer, the dipoles are parallel to each other and perpendicular to the plane of the layer. The attraction between dipoles in the head-to-tail configuration no longer appears in Eq. (12) because of the integration over the thickness of the sample implicit in the derivation of Eq. (9). Note that  $g(q=0) = 2/3$  is positive. This means that the total free energy is always stable with respect to spatially uniform fluctuations in  $\phi$ . When  $q \rightarrow \infty$ ,  $g(q)$  tends to the limit  $-1/3$  determined entirely by local fields. It is the fact that  $g(q)$  becomes negative for  $qL$  greater than a critical value that makes any transition from the spatially uniform state possible. In the absence of local fields,  $g(q)$  would be strictly positive at any finite  $q$ , so there would be no equilibrium spatially modulated phases.

Finally the Gibbs free energy  $F$  (for a chemical potential  $\mu$ ) can be expressed in terms of dimensionless lengths using the length  $\sqrt{A}$  and the transformations  $\mathbf{r} \rightarrow \sqrt{A}\mathbf{r}$  and  $q \rightarrow q/\sqrt{A}$ . The resulting dimensionless free energy  $f = (Fv_0)/(k_B T A L)$  is

$$f = \int d^2\mathbf{r} \left\{ \phi(\mathbf{r}) [f_m(m(\mathbf{r})) - m(\mathbf{r})h - \mu] + s(\phi(\mathbf{r})) + \frac{1}{2} [\nabla \phi(\mathbf{r})]^2 \right\} + 12\lambda \int d^2\mathbf{r} d^2\mathbf{r}' g(\mathbf{r}, \mathbf{r}') \phi(\mathbf{r}) \phi(\mathbf{r}') m(\mathbf{r}) m(\mathbf{r}'), \quad (13)$$

where the Fourier transform of  $g(\mathbf{r}, \mathbf{r}')$  is given by Eq. (12) with  $q$  replaced by  $q/\sqrt{A}$ . Thus,  $g(q)$  as a function of the dimensionless  $q$  is a function of  $ql$ , where  $l = L/\sqrt{A}$ .

### III. DETERMINATION OF THE PHASE DIAGRAM

We first look at a spatially uniform state of the ferrofluid. This state of the ferrofluid corresponds to a minimum of the total free energy  $f$  at  $m = \bar{m}$  and  $\phi = \bar{\phi}$ . It is obtained from the equations

$$\frac{\partial f}{\partial m} = 0 \quad \text{and} \quad \frac{\partial f}{\partial \phi} = 0. \quad (14)$$

The first of these equations yields

$$\bar{m} = \mathcal{L}(h_e),$$

with

$$h_e = h - 24\lambda g(0) \bar{\phi} \bar{m}. \quad (15)$$

The second equation determining  $\bar{\phi}$  must in general be solved numerically. It can however be solved exactly for the lattice-gas model. The result is

$$\bar{\phi} = \frac{1}{1 + \exp(-\mu) h_e / \sinh(h_e)}. \quad (16)$$

Equations (15) and (16) reproduce the main results of the model of Sano and Doi [14] and Cebers [15] for a spatially uniform ferrofluid, when  $g(0)$  is replaced by  $g(q \rightarrow \infty)$  in Eq. (15). In our problem, however,  $g(0)$  is always positive so that there is no instability toward the formation of coexisting homogeneous phases.

Spatially nonuniform configurations can be studied by expanding the free energy difference  $\Delta f(\phi, m) = f(\phi, m) - f(\bar{\phi}, \bar{m})$  in powers of  $\delta m = m(\mathbf{r}) - \bar{m}$  and  $\delta \phi = \phi(\mathbf{r}) - \bar{\phi}$ . The quadratic part of this free energy difference  $\Delta f_{quad}$  has a simple form in terms of the 2D Fourier transform  $\delta m(\mathbf{q})$  and  $\delta \phi(\mathbf{q})$ ,

$$\Delta f_{quad} = \int \frac{d^2\mathbf{q}}{(2\pi)^2} \left[ \frac{1}{2} r_{11} |\delta m(\mathbf{q})|^2 + \frac{1}{2} r_{22} |\delta \phi(\mathbf{q})|^2 + r_{12} \delta m(\mathbf{q}) \delta \phi(-\mathbf{q}) \right], \quad (17)$$

with

$$r = \begin{pmatrix} 24\lambda g(q) \bar{\phi}^2 + f_m''(\bar{m}) \bar{\phi} & 24\lambda g(q) \bar{m} \bar{\phi} \\ 24\lambda g(q) \bar{m} \bar{\phi} & 24\lambda g(q) \bar{m}^2 + s''(\bar{\phi}) + q^2 \end{pmatrix}. \quad (18)$$

The coefficient  $r_{22}$  is the most important term determining at what values of  $\lambda$  transitions occur, and it is worth investigating it in more detail. As already discussed,  $g(q)$  decreases monotonically from  $2/3$  to  $-1/3$  as  $q$  increases from  $0$  to  $\infty$ . Since  $q^2$  grows monotonically with  $q$ ,  $24\lambda g(q) \bar{m}^2 + q^2$  has a minimum at  $q = q^*$ . When  $q^* l \gg 1$ ,  $g(q) \sim 1/ql - 1/3$ , and  $q^*$  can be evaluated analytically,

$$q^* = \left[ \frac{12\lambda}{l} \mathcal{L}^2(h_e) \right]^{1/3}. \quad (19)$$

The only negative term in  $r_{22}$  is  $-\lambda/3$  coming from the local field term in  $g(q)$ . Thus, we can write in general that

$$r_{22}(q^*) = 8\bar{m}^2(\lambda_c - \lambda), \quad (20)$$

where

$$\lambda_c = \frac{1}{8\bar{m}^2} [3q^{*2} + s''(\bar{\phi})], \quad (21)$$

when  $q^* l \gg 1$ . From this, we can see that the system becomes unstable to the formation of modulated phases as  $\lambda$  grows.

The spatially uniform phase becomes globally unstable with respect to the formation of modulated phase when the determinant  $J(q) = r_{11}(q)r_{22}(q) - r_{12}^2(q)$  of the matrix in Eq. (18) evaluated at its minimum over  $q$  becomes negative. A significant simplification of the theory results when fluctuations in  $m$  are effectively frozen out, which occurs at  $\bar{m} = 1$  when  $f_m''(\bar{m}) = \infty$ . In this ideal limit, only  $\phi$  varies spatially in modulated states, and the stability of the uniform state is determined entirely by  $r_{22}(q)$  rather than by  $J(q)$ . As long as

$r_{11}(q) > 0$ , an effective theory in terms of  $\phi_q$  alone can be obtained by integrating over fluctuations in  $m$ . Removing  $m$  will lead to renormalization of the coefficients of  $(\delta\phi)^n$  for all  $n$ , as shown in Appendix B. The term with  $n=2$  is the most important for the determination of the phase diagram. Its value in the effective theory is

$$r(q) = r_{22}(q) - \frac{r_{12}^2(q)}{r_{11}(q)} \approx r_{22}(q) - \frac{[24\lambda g(q)\bar{m}]^2 \bar{\phi}}{f_m''(\bar{m})}, \quad (22)$$

where the later form is valid provided that  $f_m''(\bar{m}) \gg 8\lambda \bar{\phi}$ . The second term in this equation leads to a small shift in  $q^*$ , the most unstable wave number from its value determined by  $r_{22}(q)$  alone [Eq. (19) for  $q^*l \gg 1$ ], and to a small shift in  $\lambda_c$ , the critical value of  $\lambda$ . These shifts are small when  $\bar{m}$  is sufficiently close to 1. For instance, for  $\lambda = 0.578$ ,  $l = 1000$ , and  $\bar{\phi} = 0.5$ , the second term is much smaller than the first by at least two orders of magnitude for  $h > 14.2$ , which corresponds to  $\bar{m} > 0.9$ . This is verified in particular at the critical field for the transition to the modulated phases, which occurs in this case at  $h = 21.5$  and  $\bar{m} = 0.94$ .

For more general values of  $\lambda$  however,  $r_{11}$  can in fact become negative. Unlike  $r_{22}(q)$ ,  $r_{11}(q)$  has no stabilizing  $q^2$  term in the current theory. As a result, it reaches its minimum value of  $[f_m''(\bar{m}) - 8\lambda \bar{\phi}] \bar{\phi}$  at  $q = \infty$ . Thus if  $f_m''(\bar{m}) < 8\lambda \bar{\phi}$ ,  $r_{11}$  is negative for a range of  $q$  and  $J(q)$  will be negative for  $r_{22} > 0$ . This would indicate an instability toward a phase with very short wavelength modulations. Since our theory does not treat short wavelength physics in detail, we will consider only situations in which  $r_{11}$  is positive. In this case, an effective theory in terms of  $\phi_q$  alone can be constructed by integrating over fluctuations in  $m$ .

In constructing phase diagrams in the  $h$ - $\bar{\phi}$  plane, we have used the two models discussed above: model 1 in which the fluctuations in  $m$  are ignored, and model 2 in which they are included. Both models treat only terms up to fourth order in  $\phi_q$ . Our theory in terms of  $\phi$  only is very much in the spirit of the single order parameter theory of Cebers [15,16], except for the shifts discussed above in  $q^*$  and  $\lambda_c$ , which arise when fluctuations in  $m$  are included. We assume for simplicity that modulated phases are described by Fourier components with reciprocal lattice vectors of the smallest possible magnitude. Higher Fourier components undoubtedly can become important particularly near the hexagonal-to-stripe transition. The effects of these higher Fourier components, which are best treated using real space *Ansätze*, will be treated elsewhere. The free energy of the different phases are the following:

(1) The isotropic phase with Helmholtz free energy

$$f_{iso} = -12\lambda g(0) \bar{\phi}^2 \bar{m}^2 - \ln\left(\frac{\sinh h_e}{h_e}\right) \bar{\phi} + s(\bar{\phi}). \quad (23)$$

(2) The stripe phase with a free energy

$$f_s = f_{iso} + \frac{1}{4} r \phi_q^2 + u_s \phi_q^4. \quad (24)$$

In model 1, the stripe phase corresponds to a modulation  $\delta\phi(\mathbf{r}) = \phi_q \cos(q^*y)$ , and the coefficients in Eq. (24) are  $r = r_{22}(q^*)$  and  $u_s = s^{(4)}(\bar{\phi})/64$ . In model 2, the stripe phase is characterized by  $\delta\phi(\mathbf{r}) = \phi_q \cos(q^*y)$  and  $\delta m(\mathbf{r}) = m_q \cos(q^*y)$ . The coefficients  $r = r(h, \bar{\phi})$  of Eq. (22) and  $u_s$  of Eq. (B5) evaluated at  $q^*$  must be used.

(3) The hexagonal phase with a free energy

$$f_{hex} = f_{iso} + \frac{3}{4} r \phi_q^2 + v \phi_q^3 + u_h \phi_q^4. \quad (25)$$

In model 1, the hexagonal phase corresponds to a modulation  $\delta\phi(\mathbf{r}) = \sum_{i=1}^3 \phi_q \cos(\mathbf{q}_i \cdot \mathbf{r} + \delta_i)$  with  $|\mathbf{q}_i| = q^*$  and  $\sum_{i=1}^3 \mathbf{q}_i = 0$ . The coefficients in Eq. (25) are  $r = r_{22}(q^*)$ ,  $v = s^{(3)}(\bar{\phi})/4$ , and  $u_h = 15s^{(4)}(\bar{\phi})/64$ . In model 2, the hexagonal phase corresponds to a modulation of this type for both  $\delta\phi$  and  $\delta m$ , and the coefficients  $r = r(q^*)$ ,  $v$ , and  $u_h$  are given by Eqs. (22), (B12), and (B13).

A few comments about the general properties of our models are useful. When  $v(h, \bar{\phi})$  is zero, the free energy of the stripe phase is lower than that of the hexagonal phase as can be seen by minimizing Eqs. (24) and (25) over  $\phi_q$ . The energy density of the stripe phase at its minimum over  $\phi_q$  tends to zero as  $r^2$ , as  $r \rightarrow 0$  for  $r < 0$ . Thus, at  $\bar{\phi} = \bar{\phi}_c$  and  $h = h_c$ , determined by  $v(h_c, \bar{\phi}_c) = 0$  and  $r(h_c, \bar{\phi}_c) = 0$ , there is a second-order mean-field transition from the isotropic to the stripe phase [25]. When  $v(h, \bar{\phi})$  becomes nonzero, the hexagonal phase has lower free energy than the stripe phase at small but nonzero  $r$ . Thus, there will in general be a transition from the isotropic to the hexagonal phase away from  $\bar{\phi}_c$ , and the isotropic, stripe, hexagonal, and stripe phases will meet at the point  $\bar{\phi} = \bar{\phi}_c$ ,  $h = h_c$ . This is indeed the topology obtained in previous calculations [15–17]. The lattice-gas entropy is invariant under  $\psi = (\phi - \frac{1}{2}) \rightarrow -\psi$ , and it, therefore, only has even-order terms in a power series expansion in  $\psi$  about  $\psi = 0$ . Thus  $s^{(3)}(\bar{\phi} = \frac{1}{2}) = 0$  and the critical point in model 1 will occur at  $\bar{\phi}_c = 1/2$ . The Carnahan-Starling entropy has no reflection symmetry, and in model 1  $s^{(3)}(\bar{\phi}_c) = 0$  at  $\bar{\phi}_c = 0.1304$ . The nonentropic terms in the total free energy are not invariant under  $\psi \rightarrow -\psi$ . The result is a slight asymmetry in the phase diagram for the Carnahan-Starling model about  $\bar{\phi}_c$ . In model 2,  $\bar{\phi}_c$  and  $h_c$  can only be determined by the numerical solution of  $v(h_c, \bar{\phi}_c) = 0$  and  $r(h_c, \bar{\phi}_c) = 0$ . In our calculations, we find that this solution is in general close to the value obtained for model 1.

For a given value of the dipolar interaction parameter  $\lambda$  and the thickness  $l$ , the critical point is characterized by a critical volume fraction  $\bar{\phi}_c$  and a critical field  $h_c$ . In model 1,  $\bar{\phi}_c$  depends on the entropy only and is thus independent of the magnetic field, of  $\lambda$ , and of  $l$ . The critical field  $h_c$  on the other hand, does depend on the value of  $\lambda$  and  $l$ . In Fig. 1,

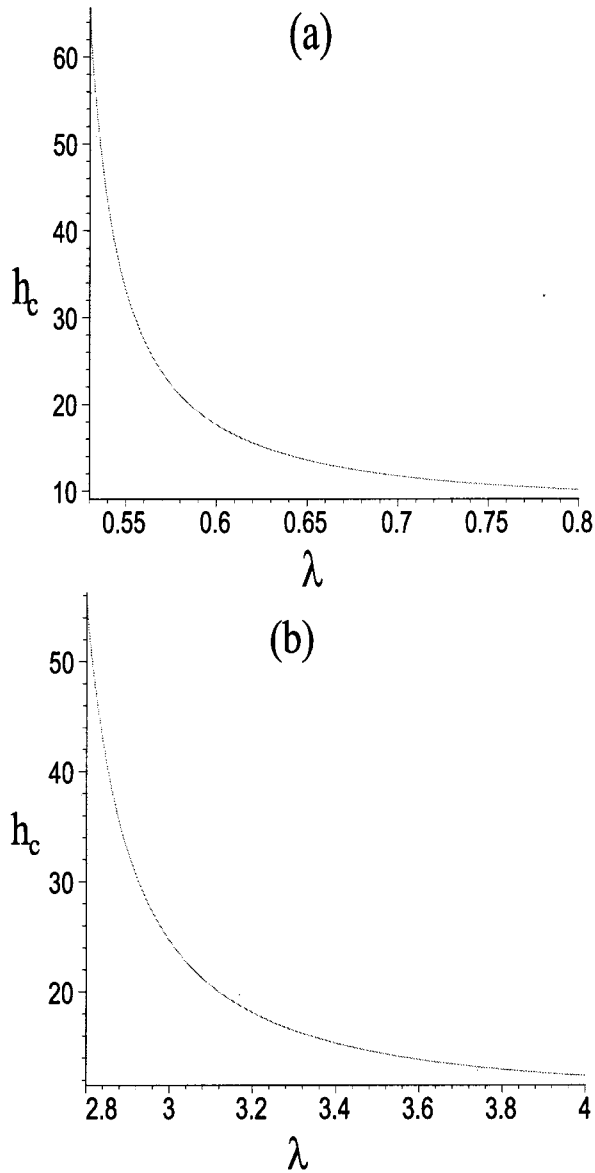


FIG. 1. Dimensionless critical field  $h_c$  as a function of the dimensionless magnetodipolar interaction parameter  $\lambda$ . Both diagrams correspond to the case of model 1 and the choice of a finite thickness of the layer  $l=1000$ . In (a) the lattice model and in (b) the Carnahan-Starling model have been used. A critical field exists only when  $\lambda$  is above a minimum value, which is 0.57 in the case of the lattice model and 2.68 in the case of the Carnahan-Starling model. Notice that the critical field  $h_c$  tends to a finite limiting value at infinite value of  $\lambda$ , which is 9.1 in the case of the lattice model and 11.32 for the Carnahan-Starling model.

the evolution of  $h_c$  in model 1 is shown as a function of  $\lambda$  for the lattice model in (a) and for the Carnahan-Starling model in (b). Both figures correspond to the choice of a finite thickness of the layer  $l=1000$ . The critical field  $h_c$  changes slightly as a function of the thickness, in this regime of large thickness where  $q^*l \gg 1$ . A critical field exists only when  $\lambda$  is above a minimum value, which is 0.57 in the case of the lattice model and 2.68 in the case of the Carnahan-Starling model. If  $\lambda$  is smaller than these limits, there are no equilib-

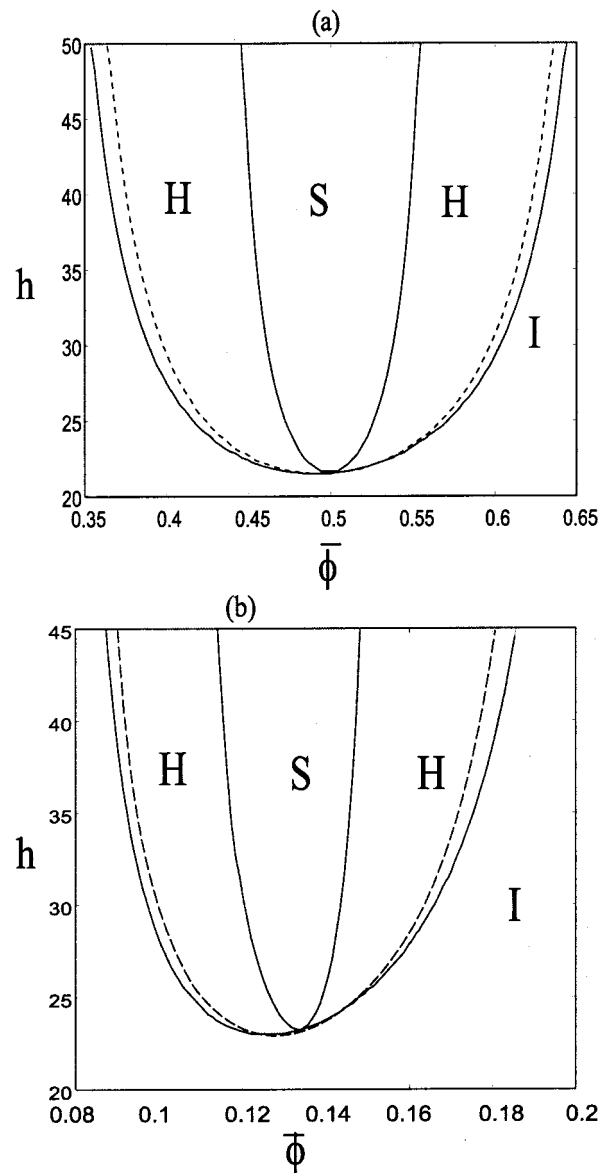


FIG. 2. Phase diagram in the  $(h, \bar{\phi})$  plane where  $h$  is the dimensionless magnetic field and  $\bar{\phi}$  is the average volume fraction of the ferrofluid.  $S$  stands for stripe phase,  $H$  for hexagonal phase, and  $I$  for uniform phase. Solid lines represent coexistence lines and the dashed line is the spinodal. (a) This diagram was obtained for  $\lambda = 0.578$ ,  $l = 1000$  with model 1 and using the entropy of a gas on a lattice of Eq. (2). (b) This diagram was obtained for  $\lambda = 3$ ,  $l = 1000$  with model 2 and using the entropy of a fluid following Carnahan-Starling equation of Eq. (3).

rium modulated phases. Notice also that the critical field  $h_c$  tends to a finite limiting value when  $\lambda$  is arbitrary large, which is 9.1 in the case of the lattice model and 11.32 for the Carnahan-Starling model. These lower bounds on the critical field are not zero, since there can be no modulated phases at zero field in this model as noted before.

Figure 2 presents phase diagrams obtained by minimizing the free energy for the different phases. In these diagrams, the spinodal line  $J(q^*)=0$  is dashed and the coexistence lines are solid. Figure 2(a) is the phase diagram for model 1

for  $\lambda=0.578$  and  $l=1000$  of a system with the lattice-gas entropy of Eq. (2), whereas Fig. 2(b) is the phase diagram for model 2 for  $\lambda=3$  and  $l=1000$  of a system with the entropy of a Carnahan-Starling fluid [12], defined in Eq. (3). In the vicinity of the critical point, all phases are present: the uniform phase ( $I$ ) (liquid on one side and gas on the other side), the hexagonal phase ( $H$ ) (direct hexagonal on one side and inverted hexagonal on the other), and the stripe phase ( $S$ ). Figure 2(a) has a lot in common with the phase diagram obtained by Andelman *et al.* [7] for Langmuir films and by Cebers for ferrofluids [16] with some important differences. In contrast to the phase diagram of Andelman *et al.*, we find that at high values of the magnetic field (which corresponds to the magnitude of the electrostatic dipolar interaction in their case), a ferrofluid of volume fraction close to  $\bar{\phi}_c=0.5$  has always periodic order. The disappearance of the stripe and hexagonal phases in the phase diagram of Andelman *et al.* was due to the breakdown of the expansion of the free energy away from the critical point. In agreement with predictions by Halsey [17] and Cebers [16], we find that the stable ordered phase of a ferrofluid at low concentration should be the hexagonal phase at low magnetic field and the stripe phase at higher magnetic field.

Figure 2(b) shows the phase diagram based on the Carnahan-Starling description of a liquid of hard spheres, which is more accurate than the lattice-gas or the Van der Waals models. For this figure, a value of  $\lambda=3$  was chosen. This is the estimated value for a monodisperse suspension of magnetite particles with  $M_s=446$  kA m<sup>-1</sup>,  $a=7.4$  nm and  $\delta=1$  nm at room temperature. For these particles,  $h$  is equal to 1 for a field of 52 G. The dimensionless length  $l$  is estimated to be 1000, which corresponds to a modulation period of 1  $\mu$ m, for  $L=40$   $\mu$ m and a magnetic field  $H=300$  G. This magnetic field is the theoretical critical magnetic field for microphase separation at a volume fraction of about 1%. As  $\lambda$  is increased further, the phase diagrams of Figs. 2(a) and 2(b) are shifted to lower fields and the modulated phases extend further away from  $\bar{\phi}_c$ . Quantitative comparison between theory and experiments require an estimate of  $\lambda$ , which presuppose precise determination of particle size and low polydispersity, as  $\lambda$  is proportional to the volume of the magnetic particles.

In our model, we have found that the hexagonal phase can coexist with the uniform phase and the hexagonal phase can coexist with the stripe phase, but the stripe phase cannot coexist with the uniform phase except at the critical point. The size of the coexistence regions of  $H+I$  and  $H+S$  have been found in our calculations to be small for both the lattice model and the Carnahan-Starling model [typically of the order of 0.01%–0.1% in volume fraction in Figs. 2(a) and 2(b)]. For higher values of  $\lambda$ , however, the width of the coexistence region of  $H+S$  becomes larger. In contrast, Refs. [7] and [16] find rather large coexistence regions, for both  $H+S$  and  $H+I$ , whose origin can be traced to the use of a power-law expansion of the free energy near a critical point in terms of the uniform part of the particle volume fraction rather than the full free energy in terms of this variable. But very close to the critical point, our theory agrees with that of Refs. [7] and [16].

#### IV. CONCLUSION

In this paper, we have presented a picture of the microphase separation and the formation of ordered phases in ferrofluids under a magnetic field using mean-field theory and a model of hard spheres for the nondipolar interaction. Within these hypotheses, we have shown that the attractive part of the dipolar interaction due to the local field is responsible for the microphase separation. In our model, this microphase separation is not possible at zero magnetic field however large the value of  $\lambda$ , in agreement with numerical simulations on the dipolar hard sphere liquid by Stevens and Grest [22,23]. Of course this conclusion would be changed if a sufficiently strong isotropic attraction was added, as in the model of Sano and Doi [14].

We have introduced a theory for phase transitions in pure ferrofluids based on two order parameters. At sufficiently high field, where the fluctuations of the magnetic moment of the particles are small, an effective theory based only on the volume fraction as an order parameter may be constructed. At infinite magnetic field, the effective theory is identical to the theory based on a single order parameter. We have compared our approach with the work of Cebers [15,16] and found essentially good agreement, with some differences which have been discussed. In order to apply our model to real ferrofluids, some knowledge of the stabilization interaction in ferrofluids due to the surfactant is needed. The modeling of this non-dipolar part of the interaction might require more than a repulsive hard core, and this will modify the condition of microphase separation and the characteristic length of the ordered phases. Thermodynamic measurements found evidence for a critical liquid-gas transition in ferrofluids, but the precise form of the nondipolar interaction is still not clear in these experiments [24]. Once the details of this interaction are known, the next step towards a better comparison with experiments will introduce polydispersity in the model, which is of importance in the context of microphase separation.

#### ACKNOWLEDGMENTS

The authors gratefully acknowledge stimulating discussions with A. G. Yodh and M. Islam. We thank A. Cebers for a careful reading of the manuscript. This work was supported in part by the MRSEC program under Grant No. NSF DMR00-79909. D.L. received support by a grant from the French Ministry of Foreign Affairs.

#### APPENDIX A: DERIVATION OF THE FUNCTION $f_m(m)$

Let  $f_m(m)$  be the free energy per magnetized particle to produce a magnetic moment  $m$ . The one particle partition function is

$$Z(h) = \frac{1}{4\pi} \int d\Omega \exp(h \cos \theta) = \frac{\sinh(h)}{h}, \quad (\text{A1})$$

where  $h$  has been defined in Eq. (6). We define  $m$  to be the angular average of the magnetic moment over all possible orientations, so that  $m = \mathcal{L}(h)$ . The free energy associated

with the partition function  $Z(h)$  is  $g(h) = -k_B T \ln[Z(h)]$ . The function  $f_m(m)$  is the Legendre transform of  $g(h)$  with respect to  $m$ :  $f_m(m) = g(h) + mh$ . This implies

$$f_m(m) = m\mathcal{L}^{-1}(m) - \ln \left\{ \frac{\sinh[\mathcal{L}^{-1}(m)]}{\mathcal{L}^{-1}(m)} \right\}, \quad (\text{A2})$$

which is the result of Eq. (5). Therefore by construction  $f_m(m)$  has the property that  $\partial f_m / \partial m = h = \mathcal{L}^{-1}(m)$ . Close to  $m=0$  the following Taylor expansion is useful:

$$f_m(m) = \frac{3}{2}m^2 + \frac{9}{20}m^4 + O(m^6). \quad (\text{A3})$$

Zhang and Widom have used the complete power series of the function  $f_m(m)$  [20]. In general  $m$  is not close to 0, and Eq. (A3) cannot be used but fortunately it is possible to calculate all the derivatives of  $f_m(m)$  analytically. For instance,

$$\begin{aligned} f_m''(m) &= \frac{\partial \mathcal{L}^{-1}(m)}{m} \\ &= \frac{-\mathcal{L}^{-1}(m)^2}{-\mathcal{L}^{-1}(m)^2 + \mathcal{L}^{-1}(m)^2 \coth^2[\mathcal{L}^{-1}(m)] - 1}. \end{aligned} \quad (\text{A4})$$

In the limit where  $m \rightarrow 1$ , which corresponds to complete alignment of the magnetic moment in the field, it is interesting to note that  $h \approx 1/(1-m)$  and  $f_m'' \approx 1/(1-m)^2$ .

## APPENDIX B: EFFECTIVE FREE ENERGY OF THE STRIPE AND HEXAGONAL PHASES

In this appendix, we give the expression of the free energy of the hexagonal and stripe phase as function of  $m_q$  and  $\phi_q$ , which are the amplitude of the spatial modulation of the two order parameters  $\phi(\mathbf{r})$  and  $m(\mathbf{r})$ . The results take a simple form when two assumptions are made: it is assumed that the coefficient of the  $m_q^2$  term  $r_{11}$  is strictly positive and that the spatial modulation of  $\phi(\mathbf{r})$  and  $m(\mathbf{r})$  are in phase with each other. With these assumptions, we derive the effective theory for  $\phi$  only, when the fluctuations of  $m$  have been integrated. Up to fourth order in  $\phi_q$  and third order in  $m_q$ , the free energy of the stripe phase is

$$\begin{aligned} f_s &= f_{\text{iso}} + \frac{1}{2}r_{11}m_q^2 + \frac{1}{2}r_{22}\phi_q^2 + r_{12}m_q\phi_q + u_1\phi_q m_q^3 + u_2m_q^2\phi_q^2 \\ &\quad + u_3\phi_q^4. \end{aligned} \quad (\text{B1})$$

The coefficients of the quadratic part have already been defined in Eq. (18), the other coefficients are

$$u_1 = \frac{1}{16}f_m'''(\bar{m}), \quad (\text{B2})$$

$$u_2 = 3\lambda g(0) + \frac{3}{2}\lambda g(2q^*), \quad (\text{B3})$$

$$u_3 = \frac{1}{64}s^{(4)}(\bar{\phi}). \quad (\text{B4})$$

Minimizing  $f_s$  with respect to  $m_q$  and reporting the result into Eq. (B1), one obtains the free energy of Eq. (24), which contains the renormalized coefficients  $r$  and  $u_s$ . The coefficient  $r$  has been defined in Eq. (22) and  $u_s$  is

$$u_s = u_2 t^2 - u_1 t^3 + u_3, \quad (\text{B5})$$

with  $t = r_{12}/r_{11}$ . The free energy at its minimum is  $(f_s)_{\text{min}} = -4r^2/u_s$ .

For the hexagonal phase, the same procedure results in the free energy

$$\begin{aligned} f_{\text{hex}} &= f_{\text{iso}} + \frac{3}{2}r_{11}m_q^2 + \frac{3}{2}r_{22}\phi_q^2 + 3r_{12}m_q\phi_q + 15u_1\phi_q m_q^3 \\ &\quad + \tilde{u}_2 m_q^2 \phi_q^2 + 15u_3\phi_q^4 + v_1 m_q^2 \phi_q + v_2 m_q \phi_q^2 + v_3 m_q^3 \\ &\quad + v_4 \phi_q^4 \end{aligned} \quad (\text{B6})$$

with

$$\tilde{u}_2 = 18\lambda \left[ 3g(0) + g(\sqrt{3}q^*) + \frac{1}{4}g(2q^*) + g(q^*) \right], \quad (\text{B7})$$

$$v_1 = \frac{3}{4}f_m'''(\bar{m}) + 36\lambda \bar{\phi} g(q^*), \quad (\text{B8})$$

$$v_2 = 36\lambda \bar{m} g(q^*), \quad (\text{B9})$$

$$v_3 = \frac{1}{4}f_m'''(\bar{m}), \quad (\text{B10})$$

$$v_4 = \frac{1}{4}s^{(3)}(\bar{\phi}). \quad (\text{B11})$$

The renormalized expression of the free energy of the hexagonal phase has been given in Eq. (25) in terms of the renormalized coefficients  $r$ ,  $v$ , and  $u_h$  with

$$v = v_4 + v_1 t^2 - v_2 t - v_3 t^3, \quad (\text{B12})$$

$$\begin{aligned} u_h &= -15u_1 t^3 + 15u_3 + \frac{2v_1 v_2 t}{3r_{11}} - \frac{v_2^2}{6r_{11}} - \frac{3v_3^2 t^3}{2r_{11}} + \frac{2v_3 t^3 v_1}{r_{11}} \\ &\quad + t^2 \tilde{u}_2 - \frac{v_3 v_2 t^2}{r_{11}} - \frac{2v_1^2 t^2}{3r_{11}}. \end{aligned} \quad (\text{B13})$$

In the limit  $m \rightarrow 1$ , the renormalized coefficients  $r, u_h, v$  tend to the value that these coefficients take in the simpler theory where the only order parameter is  $\phi$ . Indeed  $t \approx (m-1)^2$ ,  $r - r_{22} \approx (m-1)^2$ ,  $v - v_4 \approx (m-1)^2$ ,  $u_h - 15u_3 \approx (m-1)^2$ ,

and  $u_s - u_3 \approx (m-1)^3$ . Note that Eq. (B12) implies that the critical volume fraction  $\bar{\phi}_c$ , which is the solution of the equation  $v=r=0$ , is now dependent on the magnetic field. In the limit of very high field, the critical point should be identical to the critical point of the theory with  $\phi$  as the only order parameter.

In general, we have found that the phase diagram constructed from this effective theory is not very different from the phase diagram constructed with the theory based on a single order parameter. In the limit of infinite field, this effective theory becomes identical to the theory with a single order parameter (model 1).

- 
- [1] R. E. Rosensweig, *Ferrohydrodynamics* (Dover, New York, 1997).
- [2] J.-C. Bacri and D. Salin, *J. Phys. France* **43**, L771 (1982).
- [3] C.-Y. Hong, I.J. Jang, H.E. Horng, C.J. Hsu, Y.D. Yao, and H.C. Yang, *J. Appl. Phys.* **81**, 4275 (1997).
- [4] H. Wang, Y. Zhu, C. Boyd, W. Luo, A. Cebers, and R.E. Rosensweig, *Phys. Rev. Lett.* **72**, 1929 (1994).
- [5] C. Flament, J.-C. Bacri, A. Cebers, F. Elias, and R. Perzynski, *Europhys. Lett.* **34**, 225 (1996).
- [6] J. Liu, E.M. Lawrence, A. Wu, M.L. Ivey, G.A. Flores, K. Javier, J. Bibette, and J. Richard, *Phys. Rev. Lett.* **74**, 2828 (1995).
- [7] D. Andelman, F. Brochard, and J-F. Joanny, *J. Chem. Phys.* **86**, 3673 (1987).
- [8] T. Garel and S. Doniach, *Phys. Rev. B* **26**, 325 (1982).
- [9] T.E. Faber, *Proc. R. Soc. London, Ser. A* **248**, 460 (1958).
- [10] M. Seul and R. Wolfe, *Phys. Rev. A* **46**, 7519 (1992).
- [11] F.M. Ytreberg and S.R. McKay, *Phys. Rev. E* **61**, 4107 (2000).
- [12] N.F. Carnahan and K.E. Starling, *J. Chem. Phys.* **51**, 635 (1969).
- [13] K.I. Morozov, *Magnetohydrodynamics* **23**, 37 (1987).
- [14] K. Sano and M. Doi, *J. Phys. Soc. Jpn.* **52**, 2810 (1983).
- [15] A. Cebers, *Magnetohydrodynamics* **18**, 137 (1982).
- [16] A. Cebers, *Magnetohydrodynamics* **31**, 58 (1995); *Magnitnaya Gidrodinamika* **35**, 344 (1999); *Magnetohydrodynamics* **37**, 3 (2001).
- [17] T.C. Halsey, *Phys. Rev. E* **48**, R673 (1993).
- [18] P. M. Chaikin and T. C. Lubensky, *Principles of Condensed Matter Physics* (Cambridge University Press, New York, 1995).
- [19] J. P. Hansen and I. R. McDonald, *Theory of Simple Liquids* (Academic Press, New York, 1976).
- [20] H. Zhang and M. Widom, *Phys. Rev. E* **49**, R3591 (1994).
- [21] P.G. de Gennes and P.A. Pincus, *Phys. Kondens. Mater.* **11**, 188 (1970).
- [22] M.J. Stevens and G.S. Grest, *Phys. Rev. Lett.* **72**, 3686 (1994).
- [23] M.J. Stevens and G.S. Grest, *Phys. Rev. E* **51**, 5962 (1995).
- [24] E. Dubois, V. Cabuil, F. Boué, and R. Perzynski, *J. Chem. Phys.* **111**, 7147 (1999).
- [25] S.A. Brazovskii, *Zh. Eksp. Teor. Fiz.* **68**, 175 (1975) [*Sov. Phys. JETP* **41**, 85 (1975)].